NASA

Technical Memorandum 79583

The Geoid Spectrum From Altimetry

C. A. Wagner

JULY 1978

National Aeronautics and
Space Administration

Goddard Space Flight Center
Greenbelt, Maryland 20771

TM 97583

THE GEOID SPECTRUM FROM ALTIMETRY

C. A. Wagner

July 1978

GODDARD SPACE FLIGHT CENTER
Greenbelt, Maryland

THE GEOID SPECTRUM FROM ALTIMETRY

C. A. Wagner
Goddard Space Flight Center
Greenbelt, Maryland 20771

ABSTRACT

Satellite altimetry information from the world's major oceans has been analyzed to arrive at a geoid power spectrum. Using the equivalent of about 7 revolutions of data (mostly from GEOS-3) the power spectrum of the sea surface generally follows the expected values from Kaula's rule applied to the geoid.

Analysis of overlapping altimetry arcs (and oceanographic data) shows that the surface spectrum is dominated by the geoid to about 500 cycles (40 km half wavelength) but that sea state departures are significant starting at about 250 cycles (80 km).

Estimates of geopotential variances from a derived (smooth) geoid spectrum show significantly less power than Kaula's rule to about 60 cycles, but somewhat more from there to about 400 cycles. At less than 40 km half wavelength, the total power in the marine geoid may be negligible ($\ll$ 20 cm).

THE GEOID SPECTRUM FROM ALTIMETRY

C. A. Wagner
Goddard Space Flight Center
Greenbelt, Maryland 20771

ABSTRACT

Satellite altimetry information from the world's major oceans has been analyzed to arrive at a geoid power spectrum. Using the equivalent of about 7 revolutions of data (mostly from GEOS-3) the power spectrum of the sea surface generally follows the expected values from Kaula's rule applied to the geoid.

Analysis of overlapping altimetry arcs (and oceanographic data) shows that the surface spectrum is dominated by the geoid to about 500 cycles (40 km half wavelength) but that sea state departures are significant starting at about 250 cycles (80 km).

Estimates of geopotential variances from a derived (smooth) geoid spectrum show significantly less power than Kaula's rule to about 60 cycles, but somewhat more from there to about 400 cycles. At less than 40 km half wavelength, the total power in the marine geoid may be negligible ($<<20$ cm).

THE GEOID SPECTRUM FROM ALTIMETRY

INTRODUCTION

The earth and ocean dynamics application program of the National Aeronautics and Space Administration has as its goal knowledge of ocean topography at the 10 cm level (with 50 km horizontal scale). With this understanding ocean currents can be detected and calculated as departures from the mean sea surface. The shape of this mean surface is due mainly to the Earth's gravity field (the geoid) but includes contributions on a very large scale (>1000 km) from luni-solar and atmospheric tides as well as stable ocean current and wind systems. On a smaller scale there may also be stable non gravitational surface features which will be difficult to distinguish from the gravity field. But these small scale features may vary in time (meander) and be detectable by repetitive satellite altimetry. In any case the major contribution of the geoid to high frequency sea surface undulations (scale <1000 km) should be known in order to judge the importance of small scale departures and their possibility of measurement

With the advent of the satellite altimeter it is now possible to measure the spectrum of the ocean's surface to very high frequency and begin to assess these departures from the global marine geoid. Unfortunately while the spectral analysis of the sea surface from altimetry has been relatively straightforward, the interpretation of that spectrum as the reflection of a marine geoid is

ambiguous because of the uncertainty about the magnitude of the sea state (departures).

I have chosen to work out the simplest interpretation of the geoid surface using the "exterior" spherical harmonics of the geopotential for which much information is known.

In what follows, I assume the geoid is referred to a spherical surface with a radius R (637140 m). Then, using the spherical approximation of Bruns' formula (Heiskanen and Moritz, 1967, p. 85), the height of the geoid above the reference sphere is simply:

$$h = R \sum_{\ell=2}^{\infty} \sum_{m=0}^{\ell} \bar{P}_{\ell m}(\sin\phi) \left\{ C^{*}_{\ell m} \cos m\lambda + S^{*}_{\ell m} \sin m\lambda \right\} \qquad (1)$$

where ϕ is the latitude, λ the longitude, $\bar{P}_{\ell m}(\sin\phi)$ [cosm λ, sin m λ] are fully normalized spherical harmonics (Heiskanen and Moritz, 1967, p. 31) and $C^{*}_{\ell m}$, $S^{*}_{\ell m}$ are gravity coefficients of the disturbing potential. These are the usual (fully normalized) gravitational coefficients except for the lowest degree even zonals which are adjusted to discount normal gravity. However, Equation (1) is not strictly valid on the "spheroidal" surface of the ocean interior to the bounding earth sphere. Nevertheless it appears to be a reasonable first approximation [Lelgemann, 1976, p. 6].

Results from satellite tracking over the past decade have confirmed earlier gravimetric statistics that $\sigma_\ell^2 \doteq [b\ell^{-c}]^2$. ($\sigma_\ell^2$ here is the variance or mean square value of a fully normalized geopotential harmonic of degree ℓ). The constants are

$b \sim 10^{-5}$ and $c \sim 2$ consistent with theoretical expectations [Jeffreys, 1959; Cholshevnikof, 1965]. The satellite results are global but extend only to about degree 20 [e.g., Gaposchkin, 1974; Wagner et al., 1977]. The gravimetric results are far from global but are sensitive to degree 180 [e.g., Kaula, 1959; Tcherning and Rapp, 1974]. As will be seen, the detailed high degree spectrum of the geopotential from the limited 1° gravimetry used by Tcherning and Rapp appears to be too powerful. The 1° gravimetric geoid computed from considerably more data by J. Marsh (personal communication, 1976) and the altimeter geoid considered here have significantly less high degree power. Indeed even the limited sea surface heights already available from GEOS-3 (mainly) permit a confident extension of the geopotential spectrum to at least degree 400 (50 km half wavelength).

DATA ANALYSED

Forty-seven arcs of altimetry from Skylab and GEOS-3 have now been examined (Fig. 1 and Table 1). They are mostly more than 10 minutes (4500 km) long. For Skylab, the 83-minute "round-the-world" pass of 31 January 1974 was used [McGoogan, Leiteo and Wells, 1975]. However, since it was broken by 20 one minute operation pauses and a long pass over the United States, only 50 minutes of it represents actual sea-surface altimeter data. In the gaps I have interpolated data from the Marsh gravimetric geoid as I have also done to make continuous data spans in gaps of GEOS-3 altimetry.

Ten arcs of GEOS-3 altimetry (William Wells, private communications, 1976), as well as that for Skylab, were in the form of strip charts of sea surface height calculated from the high speed (~10 records/sec) data (e.g., Fig. 2). Here (as in all the arcs) the sea surface height was calculated from the orbit as the difference of the satellite's height above the ellipsoid and the measured altimeter height. Thus sea surface dynamics (e.g., tides and currents) as well as possible very long wave length orbit errors remain in this "measurement."

At the outset, I did not expect ocean dynamics to distort severely the gravity signal I sought from the altimetry. At low frequencies (<20 cycles/global rev.) the altimeter spectrum should be dominated by the geopotential (the geoid) and orbit errors. At intermediate frequencies (20 to 600 cycles/rev.; 150 to 5 second half wavelengths of altimetry record) the geoid should still dominate with an unknown (but probably small) amount of ocean dynamics. At greater frequencies, the noise of the instrument should begin to dominate.

Figure 2 shows a typical 10 second record of high speed (measured sea surface height) data from GEOS-3 over the North Atlantic. This record is from the "global" (low intensity) mode of altimeter operation which averages the (weak) return pulse over a "footprint" on the ocean of 8 km (~1 second). It is noted that a strong sinusoidal oscillation (~1 m rms) of about this period indeed exists in this data. It is probably due to the correlation of noisy return pulses overlapping (in successive records) from the same points on the ocean.

For the data arcs from "strip charts" I have (hand) drawn a smooth line through the mean of these "highest" frequency oscillations. I have also tried to avoid (in the "mean" line) too rapid fluctuation (> 5 m) over a 5 second interval which is probably due to sea state effects on the return signal. The result (sampled every 10 seconds for Skylab, 5 seconds for the "noisiest" GEOS-3 arcs and 2-1/2 seconds for the quietest) is a smoothed sea surface height record to the nearest 0.5 m (1 m for Skylab). The dominating noise in the "hand smoothed" record is this strip chart reading error. Extensive harmonic analysis [Wagner, 1977] has shown this residual error to be actually as low as 0.12 m (rms), about the same as in analysis of major frame average (2-3 second) data processed entirely by machine. The majority of the arcs were smoothed in this fashion (Table 1). In addition, however, I hand-edited all "odd' heights which differed (high or low) from both neighbors by more than 2 m.

The altimeter derived sea surface heights were then compared to the GEM 7 geoid, removing the effects of very low frequency orbit errors (mainly) at the same time [Wagner, 1976, p. 18]. Residuals from that comparison, for the longest GEOS-3 arc examined (Norway to Equador) are shown in Figure 3. Ocean bottom profiles (Fig. 3) correlate fairly well with these high frequency residuals suggesting that simple models of the crust may explain most of these features. [Wagner (1977)] displays the residual features for 10 additional long arcs.

Comparisons of this altimetry with recent low frequency geopotential models are also revealing (Table 1). GEM 7 [Wagner, et al., 1977] is a 400 coefficient

satellite model complete to (16,16) in spherical harmonics. GEM 8 (with 650 coefficients) combines the satellite data in GEM 7 with worldwide 5° x 5° surface gravimetry strongly weighted in continental areas. It is complete to (25,25). Surprisingly, the overall fit to altimetry is poorer with GEM 8 than with GEM 7. On the other hand, when the truncation effect (above 25th degree) is accounted for in the 5° data (downweighting the best continental anomalies) a solution far more favorable to ocean altimetry is achieved. This is the GEM 10 combination solution [Lerch, et al., 1977] which is only complete to (22,22). In this model, significantly high correlations among high degree coefficients are controlled by a collocation technique.

The altimeter height residuals from GEM 7 were then subjected to an harmonic analysis in order to estimate the high frequency global power spectrum of the oceans and the geoid.

HARMONIC ANALYSIS OF ALTIMETER RESIDUALS

A line was first applied to match the end points of the residuals in each arc. (The major difficulty with "edge effects" had already been eliminated by the removal of trend and offset of the original sea heights fit to the GEM 7 geoid.) Deviations of the residuals from this end matching line produced 'periodic' data which was Fourier analysed.

The raw power spectrum (so determined) for the longest GEOS-3 arc is shown in Figure 4. [Additional individual arc spectra are found in Wagner, 1977]. The power here and following is the root mean square harmonic variation.

Also shown in Figure 4 is the expected raw power for this arc due to a geopotential with degree variances following Kaula's rule [Kaula, 1966]. This expected power for a global arc of data is given closely by $70.8\ n^{-1.52}$ meters, where n is in cycles per revolution (Wagner, 1977, p. 26). For the sub global arc of (1/N) revolutions I have estimated here and following that the power in each arc harmonic is $\sqrt{N}$ times the equivalent global value (Wagner, 1977, p. 10). The most interesting aspect of this arc spectrum is its close adherence (on average) to Kaula's rule. Also, the power at low frequencies ($n < 100$ cycles per rev.) tends to be less than the rule. Power above about 100 cycles tends to be greater than the rule. However some of this increased power is due to the influence of noise above about 300 cycles. This same behavior is evident for all the individual arcs.

Figure 5 shows the discrete spectra for the 47 arcs of data together. Again there is a clear tendency for sea surface power to cross Kaula's rule from low to high frequencies. When the aggregate spectrum is averaged (rms) in groups of 10, 40 and 80 cycles (for $n > 400$ cycles/rev.), this trend is dramatically confirmed (Fig. 6). A high frequency "white" noise tail in these group averaged statistics is clearly seen in this data at about 0.7 cm/global frequency. This corresponds to an average total noise content of about 1/4 meter in each arc. Actually a second "tail" of about 0.9 cm/frequency exists at around 600 cycles,

due to the 11 hand smoothed arcs which were sampled every 5 seconds. All the power averages, P, are assumed to be made up of signal P_s, and "white" noise P_{wn} equal to these tail values, such that: $P_s^2 = P^2 - P_{wn}^2$. The original and reduced (of "white" noise) averages are both shown in Figure 6.

The ocean power statistics (reduced of noise) seem remarkably stable and compatible with a simple 2 or 3 parameter log-log law:

$$P_n = An^{B + C \log_e n}. \tag{2}$$

A least squares fit of Equation (2) to the ocean power data ($20 < n < 1000$ cy/rev.) yields:

$$A = 206\,\text{cm},\ B = -0.155,\ C = -0.199. \tag{3}$$

A simpler, but less satisfactory fit gives

$$A = 21.51\,\text{m},\ B = -1.229.$$

As further evidence of the stability (or global nature) of this solution, Figure 7 shows the same group statistics for 32 short arcs (on average) and 27 relatively long arcs, chosen arbitrarily. Most of the group statistics overlap within 2σ even to the highest frequencies. However, there does seem to be a systematic trend towards somewhat lower power ($n > 20$) in the Indian Ocean.

The spectrum of the geoid can now be found if the sea state departures (and their spectrum) can be estimated.

THE SPECTRUM OF GEOID DEPARTURES AND THE GEOID

The horizontal spectrum of all the departures from the geoid has never been studied in detail, but much is known about the individual components [e.g., Kapp, 1975, and Apel, 1976]. For example, Hendershott (1972) has given a simplified global solution for the principal lunar tide with maximum amplitudes of 1 meter requiring surface harmonics only up to (12,12). Higher surface harmonics for the full tidal function seem to have significantly smaller amplitudes [e.g., Musen and Estes, personal communication, 1977]. Significant geoid departures with short wavelengths ($n > 20$ cycles/rev.) may be associated with near-coast tides, atmospheric pressure (the "inverted barometer") and certainly with ocean current systems.

I have calculated the departure spectrum along the tracks of GEOS-3 revs. 197, 538, 259 and 260 for the average sea surface topography (due to currents) in the North Atlantic. This surface has been estimated from density measurements by Defant [1961; shown in Apel, 1976]. The group averaged high frequency spectrum for these tracks (after subtracting an end-matching trend) is shown in Figure 8. The estimated effects are a full order of magnitude below the power from Kaula's rule for the geoid. However these departures are long term averages and may underestimate the profile at the time of the altimeter pass. To find these, the time varying effects, I have analysed the height differences in 9 overlapping pairs of GEOS-3 altimeter arcs. Each arc of the overlap-pair is separated from its twin by multiples of 37 days (526 orbits). Two of

these pairs contain an arc that passes close to the "eye" of a North Atlantic hurricane ["Gladys"; 2 Oct., 1975]; four pairs have close-to-shore segments. The group average results are also shown in Figure 8, reduced of (estimated) noise and scaled down (by $\sqrt{2}$) to estimate the departure effect on each arc of an overlapping pair.

There does seem to be considerably more power in the "active" departures ($n > 20$) than in the averaged ocean topography. In fact the decline of departure power appears to be very slow ($40 < n \lesssim 600$) compared to the total sea surface spectrum. Finally in Figure 9 I have estimated the global geoid power as:

$$P_n^2 = [< P_n \text{ (sea surface heights)} > - P_n^2 \text{ (departures)}] . \qquad (4)$$

Beyond 600 cycles no data is given because of the large uncertainty in the effects of departures. A fit of the 3 parameter power law (3) to this geoid data is quite satisfactory yielding:

$$A = 94 \text{ cm.}, \; B = -0.235, \; C = -0.168 \qquad (5)$$

GEOPOTENTIAL VARIANCES

Using the results of Wagner [1977, Equation (11)] individual geopotential variances σ_ℓ^2 can be found from the "one dimensional" geoid power spectrum providing global arcs of data have been taken. In the absence of such data (as here), probably only trends or group averaged variances can be so determined. These trends for the high degree variances implied by the smooth residual geoid

power law (5) are shown in Figure 10. I have also compared these variances to group averages derived from Tscherning and Rapp's (1974) 1° covariance function of gravimetry. As Figure 10 shows, the detailed gravimetric variances ($25 < \ell < 140$) appear too high compared to those derived here from altimetry and from a global set of 5° mean gravity anomalies (Rapp, 1977). The altimetric results seem to be natural extensions of recent geopotential determinations from satellite and surface data.

SUMMARY AND CONCLUSIONS

Preliminary estimates of the global spectrum of the sea-surface and geoid have been made using altimeter data from the GEOS-3 and Skylab spacecraft. In all, the equivalent of about 7 revolutions of data has served for the "global" estimates. The total power in the sea surface topography at and above 20 cycles/revolution (<1000 km half wavelength) is 2.18 m (rms). The power above 220 cycles (<91 km half wavelength) is 0.33 m (rms). The sea surface power departs noticeably above the best estimate of the geoid power at all frequencies higher than 400 cycles. The "departure" spectrum itself is relatively constant between 40 and 600 cycles. Above 500 cycles (<40 km half wavelength) the geoid power may be negligible.

The geoid power above 20 cycles from Kaula's rule is 2.38 m (rms). Thus the altimeter residuals overall, are compatible with geopotential variances somewhat less than $10^{-5}/\ell^2$. These variances appear to be less than Kaula's rule for $\ell \leq 60$ and possibly for all degrees greater than about 500.

The geopotential interpretation of the "measured" marine geoid power spectrum here assumes the geoid undulations are (essentially) the same as potential variations on the bounding earth sphere. No adequate alternative representation is available for the conventional exterior potential (in spherical harmonics) on the interior geoid surface.

ACKNOWLEDGMENTS

I thank Jeanne Roy for many of the harmonic analyses and the calculation of data residuals. The detailed calibration and verification of the method of analysis benefitted greatly from stimulating discussions with Francis J. Lerch.

REFERENCES

Apel, J. R., Ocean science from space, EOS (Transactions of the American Geophysical Union) 57; 612, 1976.

Cholshevnikov, K. V., On the values of the tesseral harmonic coefficients; Vest, Univ, Leningrad, No. 13, 1965.

Defant, A., Physical Oceanography, Vol. 1, Pergamon, N.Y., 1961.

Gaposchkin, E. M., Earth's gravity field to the eighteenth degree and geocentric coordinates for 104 stations from satellite and terrestrial data, Journal of Geophysical Research 79, 5377, 1974.

Hendershott, M. C., The effects of solid earth deformation on global ocean tides, Geophys. J. Royal Astron. Soc., 29, 389-403, 1972.

Jeffreys, H., The Earth, 4th Edition, Camb. Univ. press, 1959.

Kaula, W. W., Theory of Satellite Geodesy, p. 98, Blaisdell Press, Waltham, Mass., 1966.

Kaula, W. M., Statistical and harmonic analysis of gravity, J. Geophys. Res. 64, 2401-2422, 1959.

Lelgemann, D., Some problems concerned with the geodetic use of high precision altimeter data, Ohio State Dept. of Geodetic Science Report No. 237; Columbus, Ohio, 1976.

Lerch, F. J., Klosko, S. M. and R. E. Laubscher, Gravity model improvement using geos 3 (GEM 9 & 10), EOS, 58 #6, p. 371, June 1977.

McGoogan, J. T., C. D. Leitao and W. T. Wells, Summary of Skylab S-193 altimeter altitude results, NASA TM X-69355, pp. 207-228, Wash. D. C. 1975.

Rapp, R. H., Potential coefficient determinations from 5° terrestrial gravity data, Ohio State Dept. of Geodetic Sciences Report No. 251, p. 36, Columbus, Ohio, 1977.

Rapp, R. H., The geoid: definition and determination, In: Proceedings of the geodesy/solid earth and ocean physics Research Conferences, p. 69-77, Ohio State Dept. of Geodetic Sciences Report No. 231; Columbus, Ohio, 1975.

Tscherning, C. C. and R. H. Rapp, Closed covariance expressions for gravity anomalies, geoid undulations, and deflections of the vertical implied by anomaly degree variance models, Ohio State Dept. of Geodetic Sciences Report No. 208; p. 83 & 84 Columbus, Ohio, 1974.

Wagner, C. A., The spectrum of the geoid from altimeter data, NASA-GSFC Document X-921-77-63, Greenbelt, Md., 1977.

Wagner, C. A., The accuracy of Goddard earth models, NASA-GSFC Document X-921-76-187, pp. 191, 193; Greenbelt, Md. 1976.

Wagner, C. A., F. J. Lerch, J. E. Brownd and J. A. Richardson, Improvement in the geopotential derived from satellite and surface data (GEM 7 and 8), J. Geophys. Res., 82, 901, 1977.

Table 1

Statistics of Altimeter Data and Arcs Used

Arc (GEOS-3 Rev.)	Length (Min.)	rms Sea Surface Height Residual (m) Using: GEM 7	GEM 8	GEM 10	Comment G = Global Mode Data; I = Intensive Mode Data W2 = Wallops 2 Second Averaged Data
Skylab	52.2	3.04	4.56	2.98	Hand Smoothed Data
(129)	15.6	2.58	4.96	2.84	G, Hand Smoothed Data
(166)	8.3	1.03	2.62	1.29	I, W2
(182)	11.8	4.24	3.05	3.99	W2
(197)	29.1	2.96	3.61	2.64	I, Hand Smoothed Data
(240)	17.8	2.40	2.63	2.22	W2
(259)	10.0	1.78	1.52	1.48	G, W2
(260)	9.9	4.15	3.85	3.88	W2
(301)	10.3	3.14	2.92	3.45	Hand Smoothed Data
(319)	18.2	3.07	2.79	1.99	I, Hand Smoothed Data
(324)	19.9	3.22	2.59	2.39	Hand Smoothed Data
(362)	14.4	2.12	1.91	1.57	Hand Smoothed Data
(416)	11.2	4.87	6.68	4.77	G, Hand Smoothed Data
(458)	12.4	2.06	2.69	1.02	I, W2
(528)	16.1	3.18	2.92	2.98	W2
(537)	13.9	3.65	2.16	2.02	I, W2
(538)	15.1	3.09	3.12	2.74	I, Hand Smoothed Data
(571)	18.7	1.45	3.56	2.22	I, W2
(584)	17.9	2.53	4.65	2.71	W2
(605)	21.6	2.49	3.87	2.84	I, W2
(619)	19.2	2.02	3.04	1.74	W2
(620)	23.4	2.31	3.37	1.82	W2
(632)	10.3	1.49	2.04	2.08	I, W2
(660)	21.7	1.97	3.59	1.85	I, W2
(709)	18.7	2.49	2.24	1.73	W2
(710A&B)	22.5	2.16	2.15	0.85	W2
(817)	17.4	2.56	2.66	1.86	I, W2
(826)	10.4	2.32	4.19	1.61	I, W2
(855)	17.0	2.77	4.59	2.49	I, W2
(1390)	16.5	2.86	3.17	2.56	I, W2
(1568)	10.3	2.23	2.54	1.60	I, W2
(1580)	14.7	2.07	2.44	1.46	I, W2
(1667)	12.3	1.31	2.64	1.81	W2
(1696)	10.8	2.47	2.36	1.59	I, W2
(1719)	13.4	1.55	2.38	1.56	W2
(1804)	13.6	1.79	2.69	1.50	W2
(1894)	10.2	5.26	4.82	5.87	W2
(1944)	24.3	3.02	2.57	2.36	I, W2
(1962)	24.8	1.37	1.85	2.09	I, Hand Smoothed Data
(1993)	22.2	3.32	4.72	3.45	Hand Smoothed Data
(2173)	10.7	2.68	1.66	1.66	I, W2
(3182)	21.5	3.44	2.59	2.17	I, W2
(4658)	7.0	2.66	2.50	2.11	I, W2
(4660)	7.2	1.06	2.43	0.74	I, W2
(4661)	6.5	1.30	1.31	1.51	I, W2
(4662)	11.7	2.51	1.57	1.84	I, W2
Totals:	742.7	2.73	3.31	2.45	← rms Residual (47 Arcs)

ORIGINAL PAGE IS
OF POOR QUALITY

Figure 1. Altimeter Arcs Used

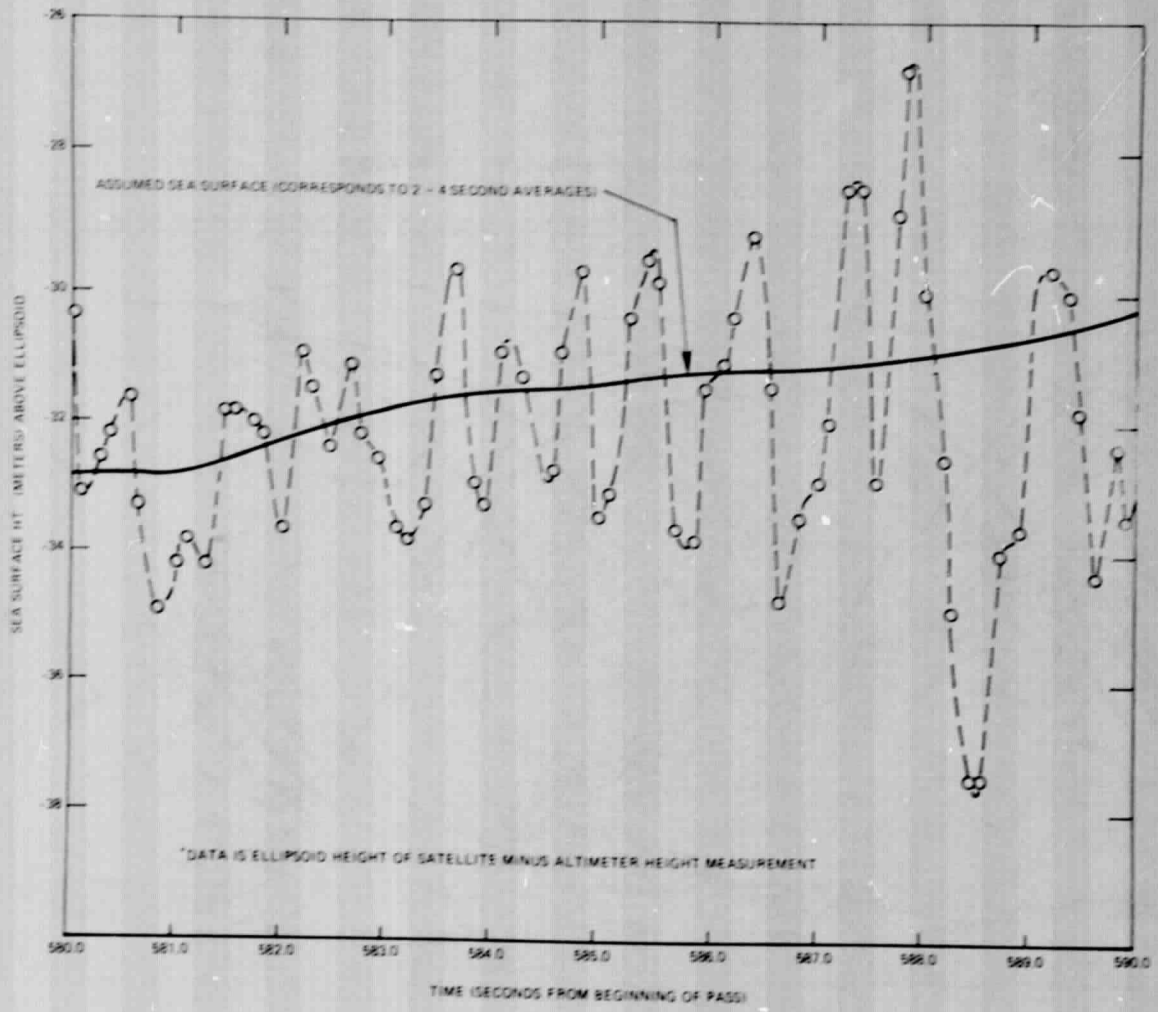

Figure 2. Sea Surface Heights Over the North Atlantic from "High Speed" GEOS-3 Altimetry*

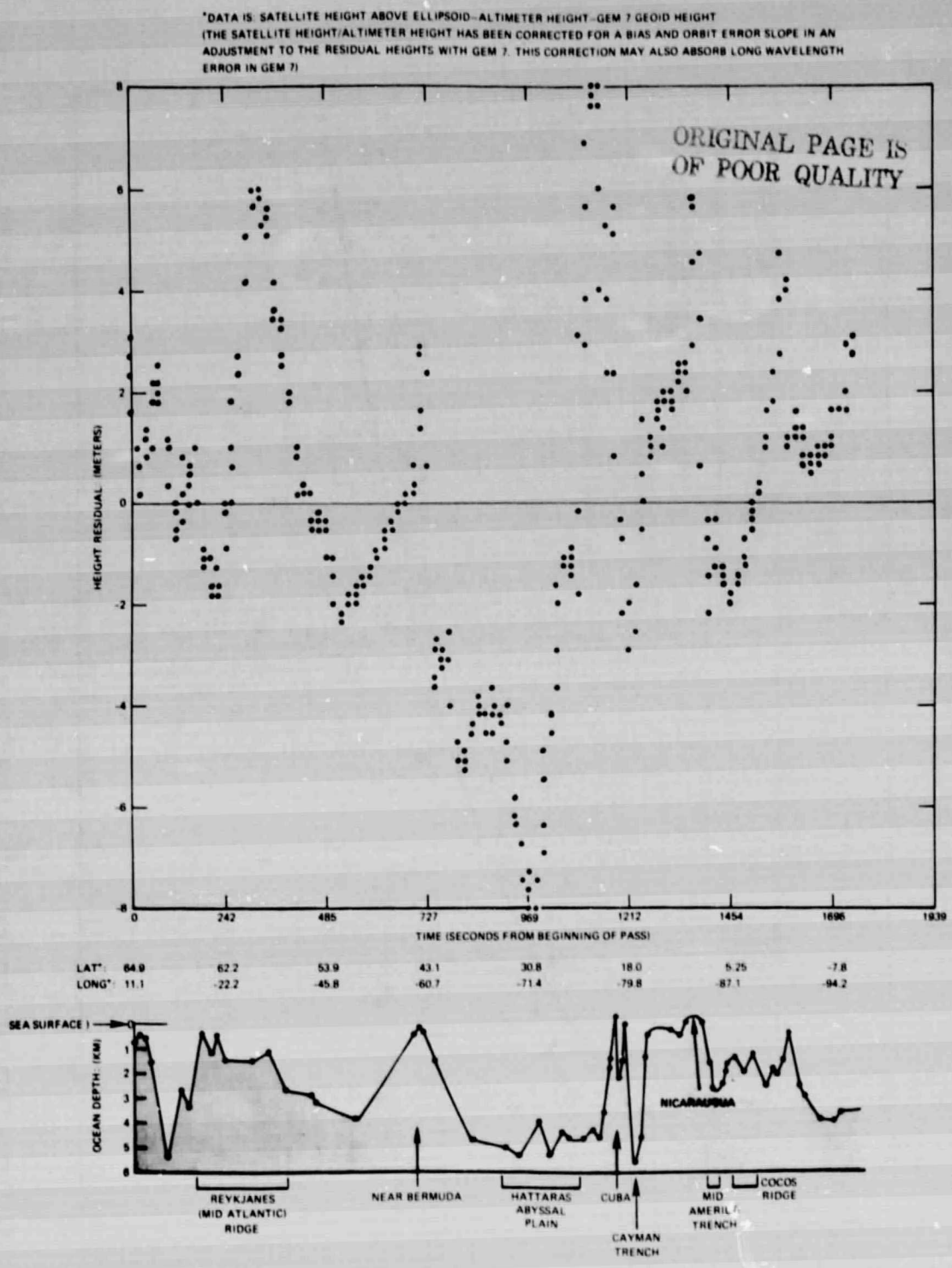

Figure 3. Sea Surface Height Residuals of Satellite Altimetry with GEM 7: GEOS-3, Rev. 197*

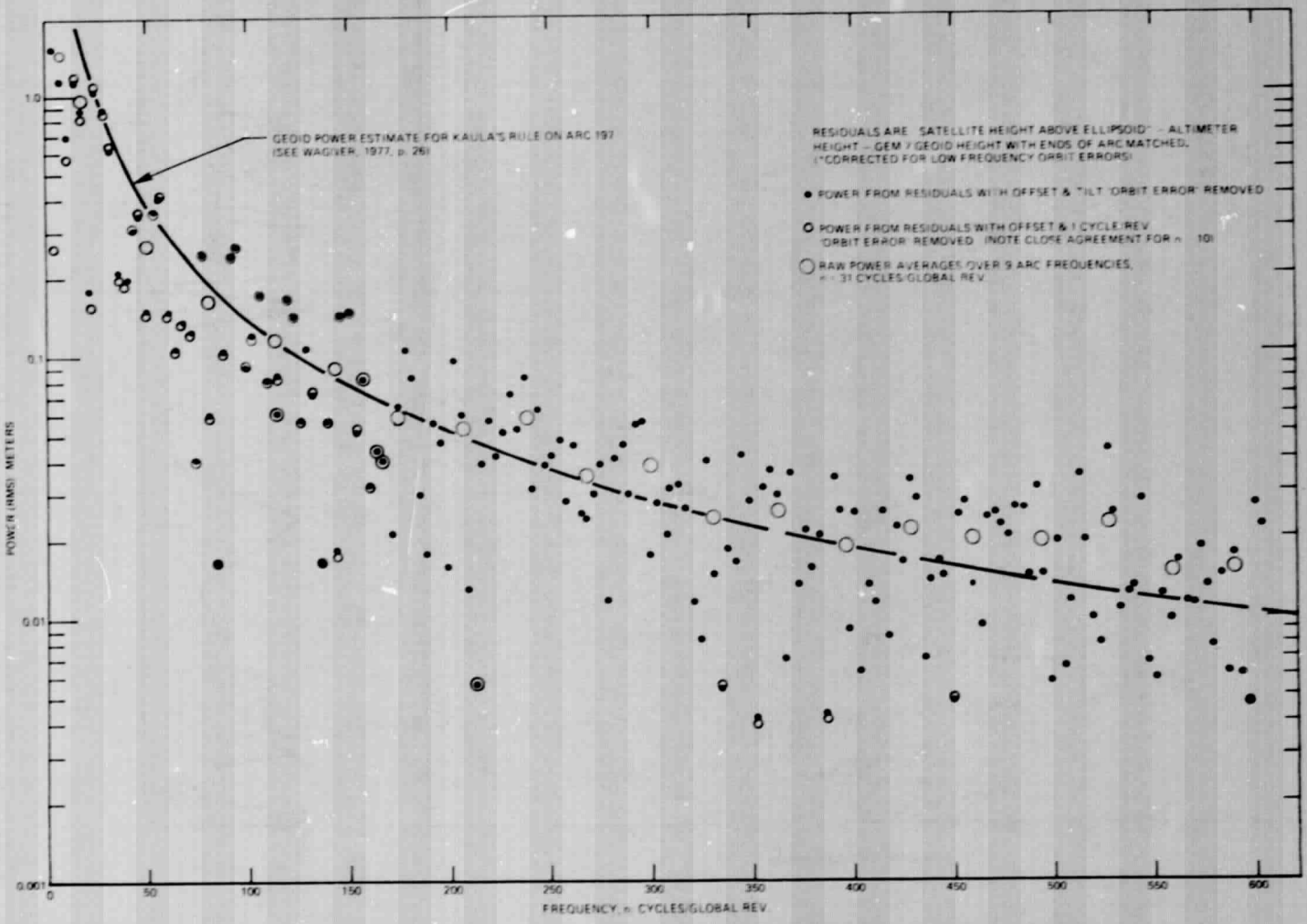

Figure 4. Power Spectrum for Sea Surface Height Residuals from Satellite Altimetry — GEOS-3, Rev. 197

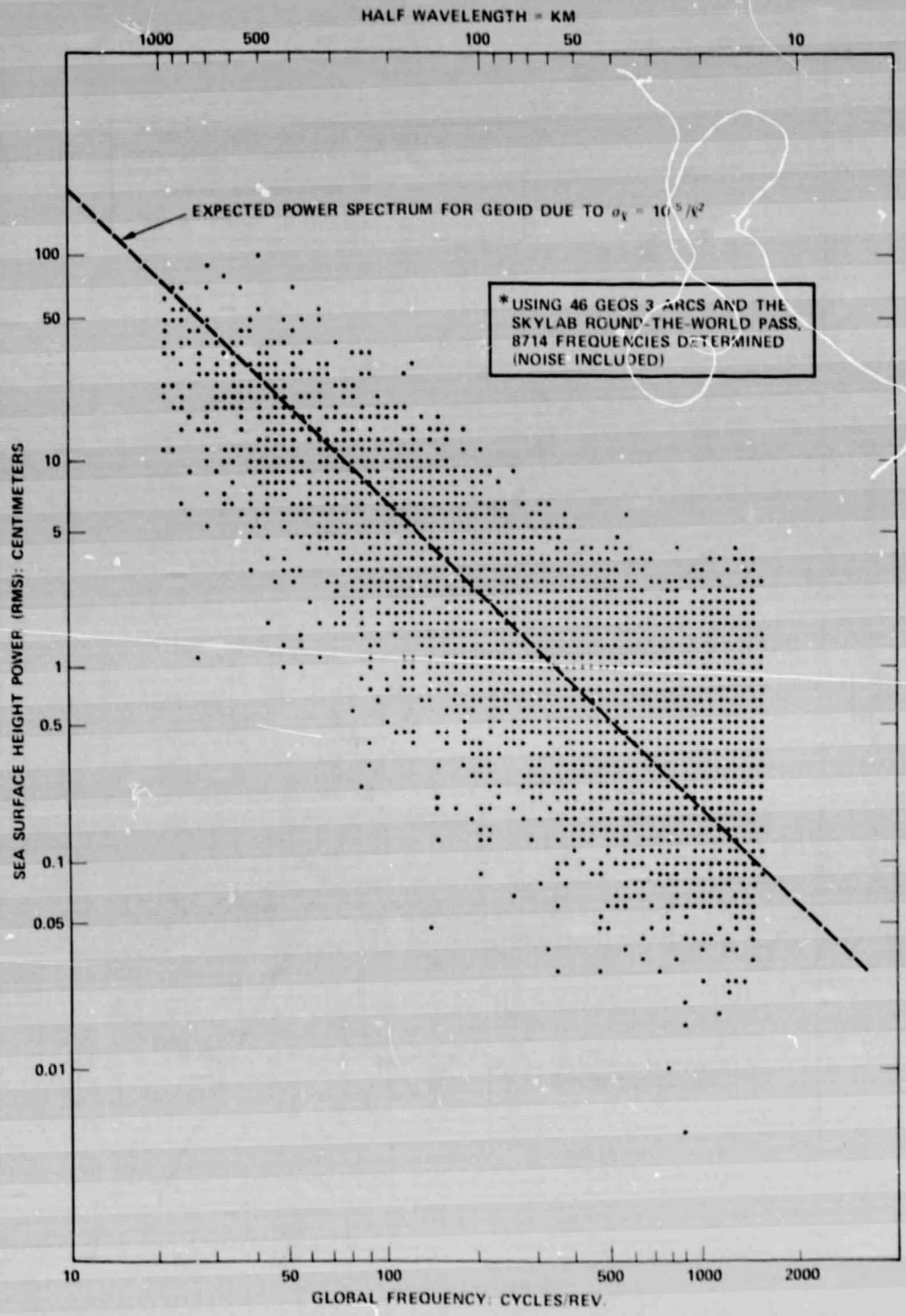

Figure 5. Sea Surface Height Power Spectrum from Altimetry*

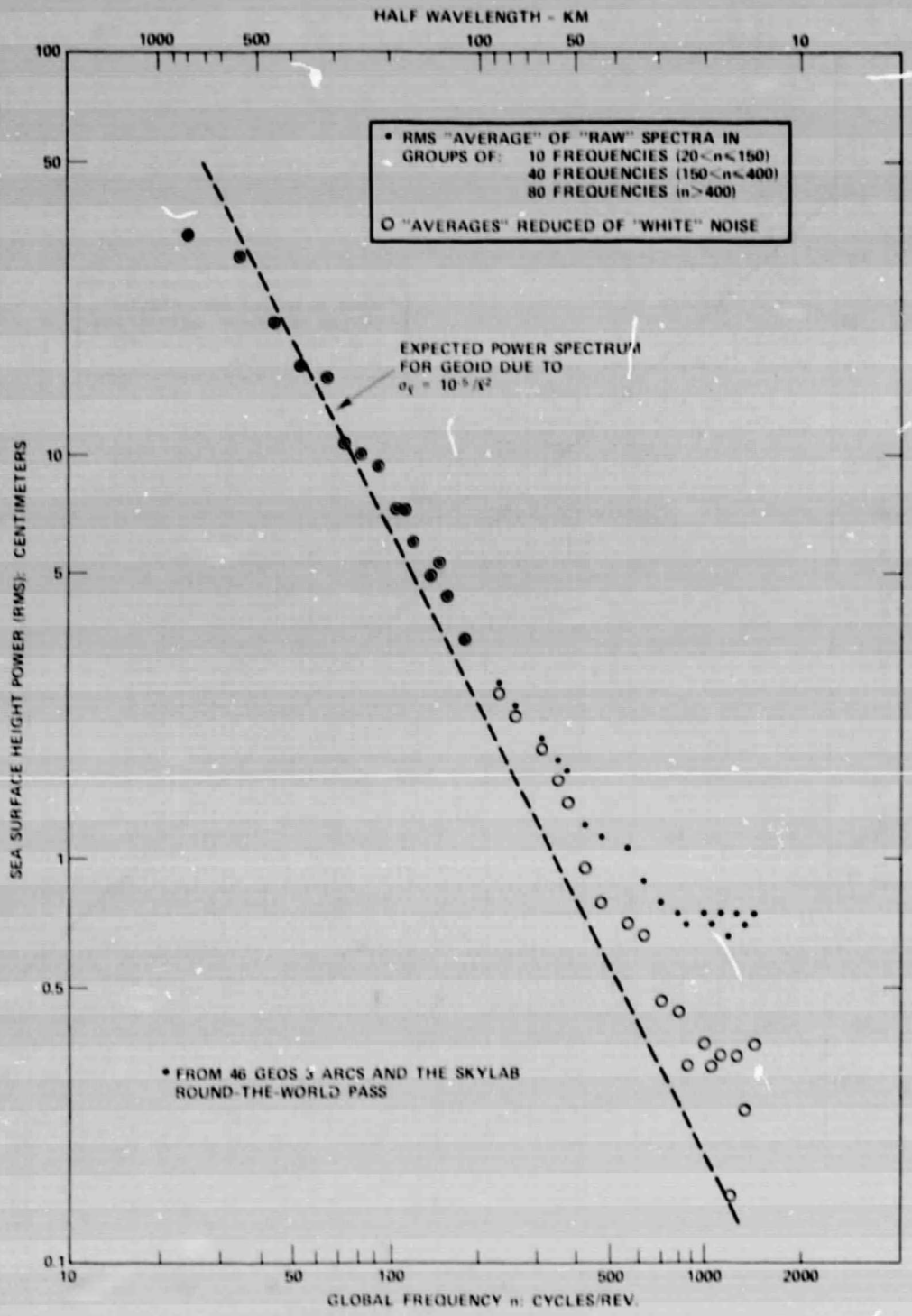

Figure 6. "Averaged" Sea Surface Height Spectrum from Altimetry*

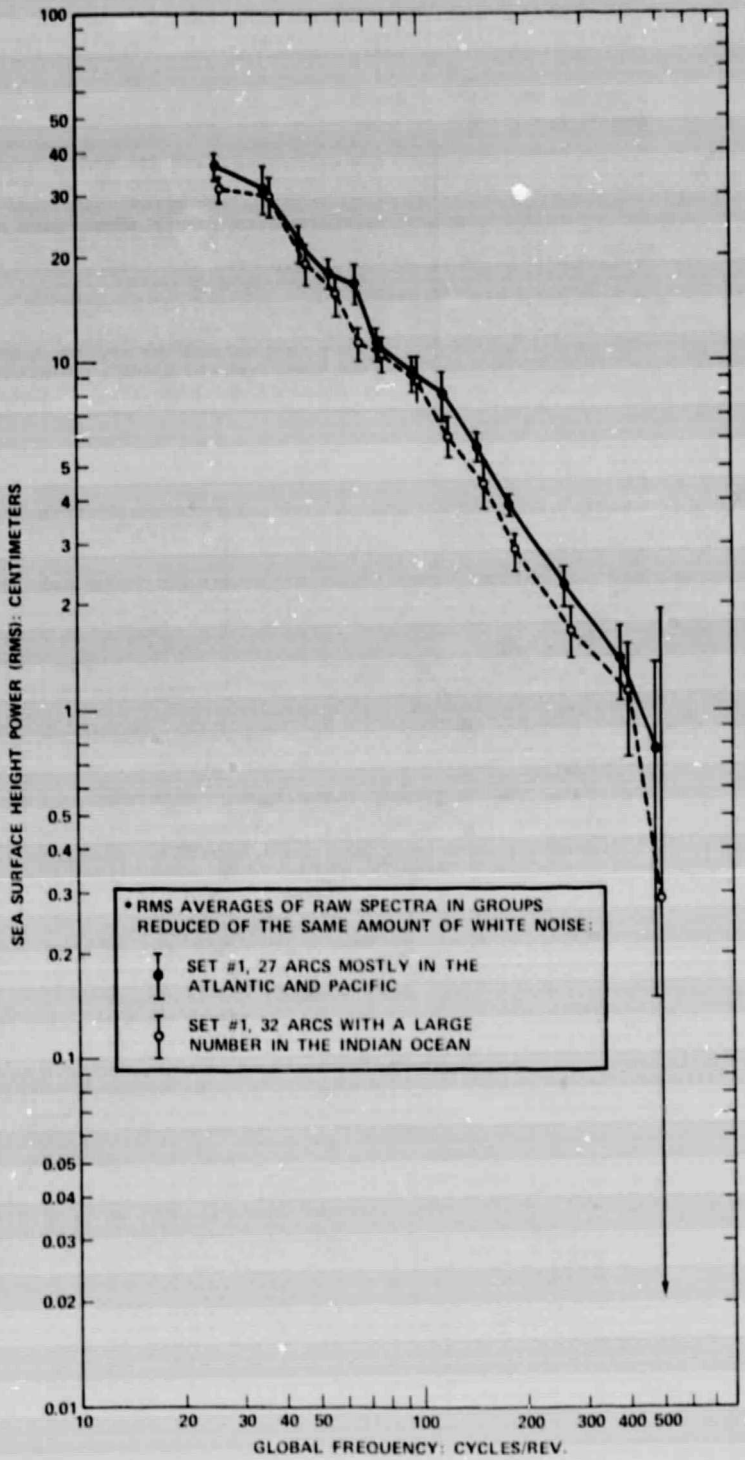

Figure 7. Comparison of Two Power Spectra from Independent Sets of Altimetry*

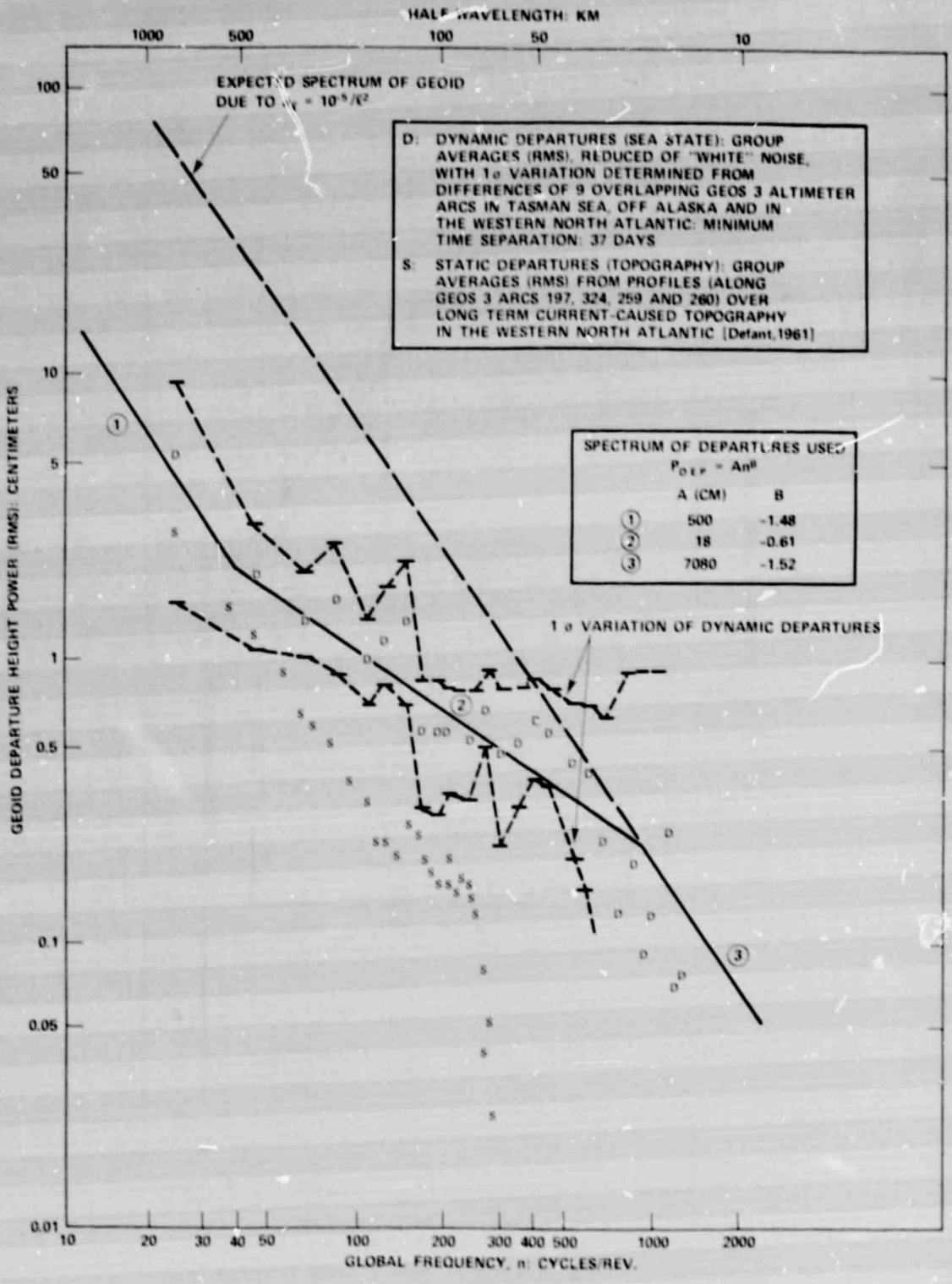

Figure 8. Spectra of Geoid Departures

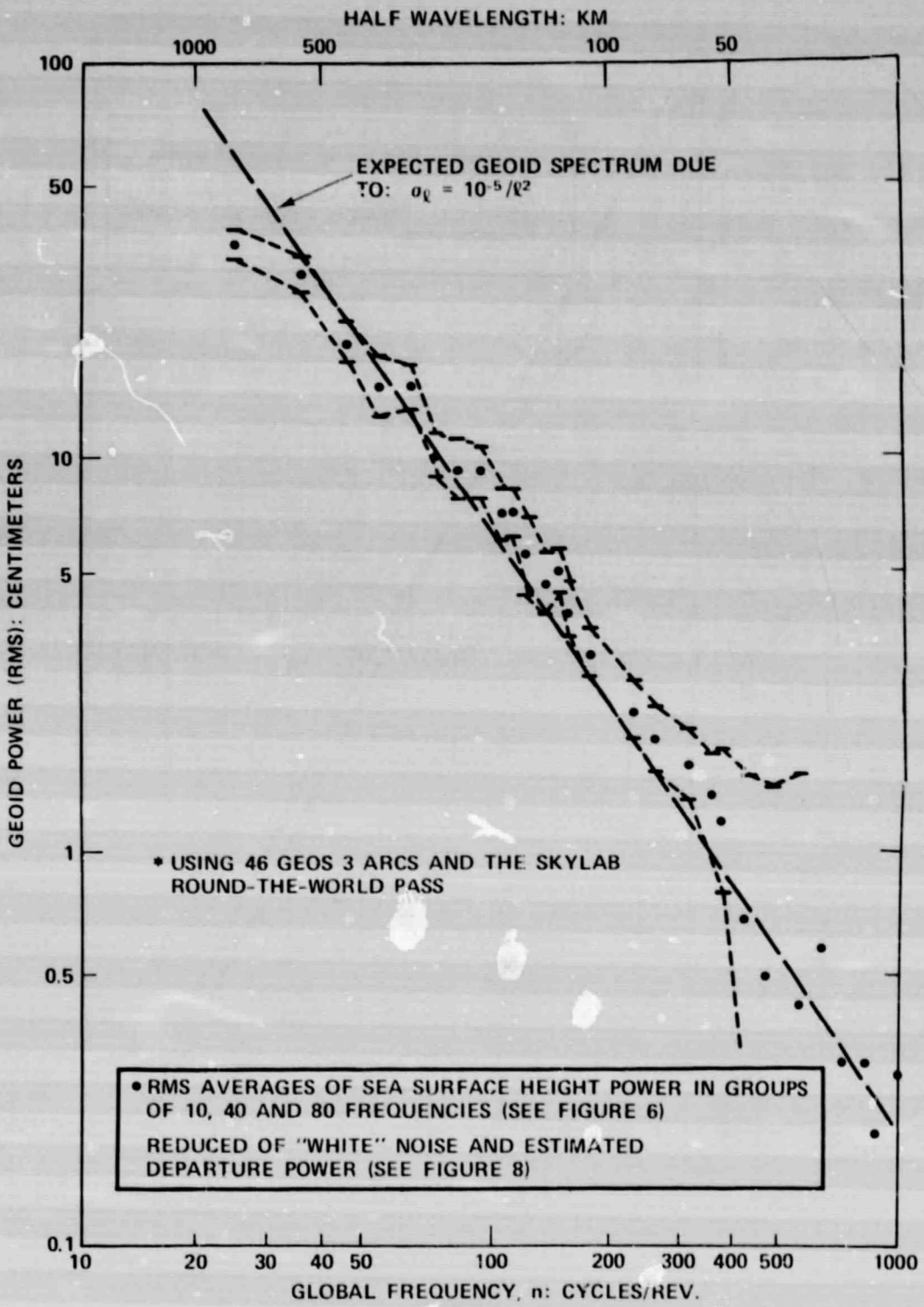

Figure 9. Power Spectrum of the Geoid from Altimetry*

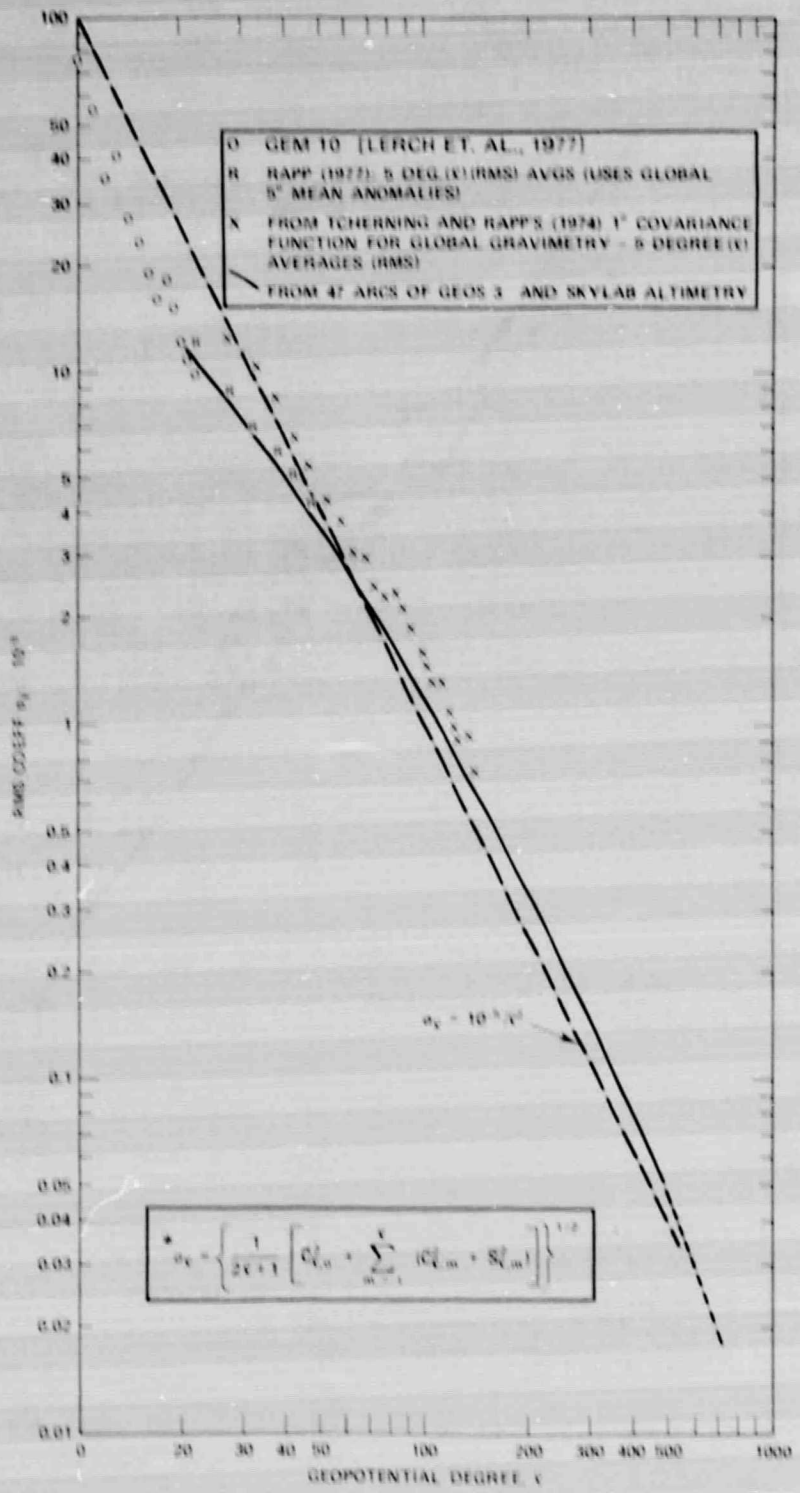

Figure 10. RMS Geopotential Coefficient by Degree*

BIBLIOGRAPHIC DATA SHEET

1. Report No.	2. Government Accession No.	3. Recipient's Catalog No.
79583		

4. Title and Subtitle	5. Report Date
The Geoid Spectrum From Altimetry	July, 1978
	6. Performing Organization Code
7. Author(s)	8. Performing Organization Report No.
C. A. Wagner	
9. Performing Organization Name and Address	10. Work Unit No.
Geodynamics Branch, Code 921 Goddard Space Flight Center Greenbelt, Maryland 20771	11. Contract or Grant No.
	13. Type of Report and Period Covered
12. Sponsoring Agency Name and Address	Technical Memorandum
National Aeronautics and Space Administration Goddard Space Flight Center Greenbelt, Maryland 20771	14. Sponsoring Agency Code

15. Supplementary Notes

To be published in Journal of Geophysical Research

16. Abstract

Satellite altimetry information from the world's major oceans has been analyzed to arrive at a geoid power spectrum. Using the equivalent of about 7 revolutions of data (mostly from GEOS-3) the power spectrum of the sea surface generally follows the expected values from Kaula's rule applied to the geoid.

Analysis of overlapping altimetry arcs (and oceanographic data) shows that the surface spectrum is dominated by the geoid to about 500 cycles (40 km half wavelength) but that sea state departures are significant starting at about 250 cycles (80 km).

Estimates of geopotential variances from a derived (smooth) geoid spectrum show significantly less power than Kaula's rule to about 60 cycles, but somewhat more from there to about 400 cycles. At less than 40 km half wavelength, the total power in the marine geoid may be negligible ($\ll$ 20 cm).

17. Key Words (Selected by Author(s))	18. Distribution Statement
Geopotential, Geoid Spectrum, Altimetry Sea Surface Spectrum, Sea Surface Topography	

19. Security Classif. (of this report)	20. Security Classif. (of this page)	21. No. of Pages	22. Price*
Unclassified	Unclassified	32	

*For sale by the National Technical Information Service, Springfield, Virginia 22151.